Photoinduced Rashba Spin-to-Charge Conversion via an Interfacial Unoccupied State

Jorge Puebla,[1,*] Florent Auvray,[2] Naoya Yamaguchi,[3] Mingran Xu,[2] Satria Zulkarnaen Bisri,[1] Yoshihiro Iwasa,[1,4] Fumiyuki Ishii,[5,6] and Yoshichika Otani[1,2,†]

[1]*CEMS, RIKEN, Saitama, 351-0198, Japan*
[2]*Institute for Solid State Physics, University of Tokyo, 5-1-5 Kashiwanoha, Kashiwa, Chiba, 277-8581, Japan*
[3]*Division of Mathematical and Physical Sciences, Graduate School of Natural Science and Technology, Kanazawa University, Kanazawa, Ishikawa, 920-1192, Japan*
[4]*Quantum Phase Electronic Center (QPEC) and Department of Applied Physics, University of Tokyo, Bunkyo-ku, Tokyo, 113-8656, Japan*
[5]*Faculty of Mathematics and Physics, Institute of Science and Engineering, Kanazawa University, Kanazawa, Ishikawa, 920-1192, Japan*
[6]*Nanomaterials Research Institute, Kanazawa University, Kakuma-machi, Kanazawa, Ishikawa, 920-1192, Japan*

At interfaces with inversion symmetry breaking, the Rashba effect couples the motion of the electrons to their spin; as a result, a spin charge interconversion mechanism can occur. These interconversion mechanisms commonly exploit Rashba spin splitting at the Fermi level by spin pumping or spin torque ferromagnetic resonance. Here, we report evidence of significant photoinduced spin-to-charge conversion via Rashba spin splitting in an unoccupied state above the Fermi level at the $Cu(111)/\alpha$-Bi_2O_3 interface. We predict an average Rashba coefficient of 1.72×10^{-10} eV m at 1.98 eV above the Fermi level, by a fully relativistic first principles analysis of the interfacial electronic structure with spin orbit interaction. We find agreement with our observation of helicity dependent photoinduced spin-to-charge conversion excited at 1.96 eV at room temperature, with a spin current generation of $J_s = 10^6$ A/m^2. The present Letter shows evidence of efficient spin charge conversion exploiting Rashba spin splitting at excited states, harvesting light energy without magnetic materials or external magnetic fields.

The Rashba effect has provided fertile ground for basic research and innovative device proposals in condensed matter. Particularly attractive is the fact that in crystals lacking spatial inversion symmetry the induced spin orbit field couples to the electrons' magnetic moment. This spin orbit coupling (SOC) allows the conversion of spin current to a transverse electrical charge, or vice versa, the conversion of an unpolarized electrical current to spin polarization and diffusion as spin current. These mechanisms have been confirmed in a variety of systems lacking spatial inversion symmetry, opening the condensed matter subfield of spin orbitronics [1,2]. Although, the first demonstration of spin charge interconversion occurred in semiconductor bulk systems, the recent focus has been the lack of spatial inversion symmetry at metal-metal, metal-semiconductor, metal-oxide, and oxide-oxide interfaces, as well as surface states in topological insulators [3]. Common techniques for exploring the spin charge interconversion phenomena at interfaces are the spin pumping and spin transfer torque ferromagnetic resonance. These techniques allow studying the conversions at occupied states below the Fermi level. Arguably, the hybridization of states at interfaces of seemingly different material systems leads to a complex modified electronic structure with multiple Rashba SOC crossings below and above the Fermi level, and even topological points. This statement has been tested by evidence showing a significant modulation of SOC as the Fermi level is increased and new states are occupied [4–6]. However, feasibility of spin-to-charge conversion via Rashba spin splitting at unoccupied states has been elusive.

In this Letter we show evidence of photoinduced spin-to-charge conversion via Rashba spin splitting of unoccupied states at the $Cu(111)/\alpha$-Bi_2O_3 interface. Recent reports showed the efficient spin-charge interconversion phenomena at the $Cu(111)/\alpha$-Bi_2O_3 interface by microwave photon spin pumping [7], acoustic spin pumping [8], and magneto-optical Kerr effect detection of current induced spin polarization [9,10]. The origin of the formation of the two-dimensional gas (2DEG) with SOC at this interface between polycrystalline layers is an ongoing topic of debate. One leading hypothesis is the formation of 2DEG by interfacial charge transfer facilitated by the presence of a significant concentration of oxygen defects, an hypothesis recently proposed as a mechanism for the formation of 2DEG at the amorphous-crystalline perovskite oxide interfaces [11]. We recently reported the properties of the two-dimensional electron gas formation in the $Cu(111)/\alpha$-Bi_2O_3 interface with spin orbit coupling by
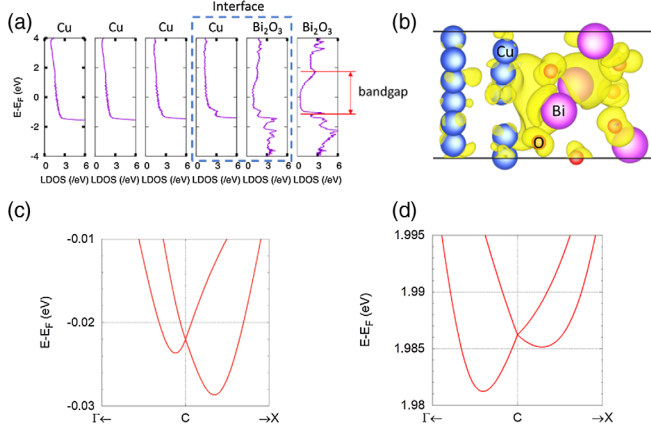
FIG. 1. First-principles analysis of the Cu(111)/α-Bi$_2$O$_3$ interface. (a) Local density of states at the Cu(111)/α-Bi$_2$O$_3$ interface (dashed line zone) and its vicinity. (b) Schematic representation of the charge density of a Rashba state around 1.98 eV above the Fermi level of the Cu(111)/α-Bi$_2$O$_3$ interface based on density functional theory. Blue spheres are copper atoms, red oxygen atoms and purple bismuth atoms; the yellow shadows show the Cu-O-Bi states. Enlarged views of the band structures around the C point are shown through each path within the range of (c) 0.02 (Bohr)$^{-1}$ and (d) 0.005 (Bohr)$^{-1}$ from the C point along the $C\Gamma$ or CX line. The origin in energy is set to be the Fermi level and there are special points: Γ (0, 0, 0); C (0.5, 0.5, 0); X (0.5, 0, 0).

FIG. 2. (a) Schematic representation of transverse photovoltaic detection following $E \approx \sigma_s \times J_s$. A laser illuminates the sample at an incidence angle θ and an azimuthal angle Ψ with polarization $\sigma^{\pm}$. (b) Helicity dependent photoinduced conversion. Photon polarization dependence of transverse photovoltage of Cu(111)/α-Bi$_2$O$_3$ at incidence angle $\theta = 70°$ and azimuthal angle $\Psi = 0°$. Open black circles represent the data and the dashed black line the fit following Eq. (1). The blue dashed line shows the linear polarization contribution (L_1). The red line shows the circular polarization contribution (V_C). The green dashed line shows the photovoltage related to Fresnel factors (L_2).

spectroscopic ellipsometry [12]. Polycrystalline interfaces have the advantage of reduced interfacial strain and higher carrier concentrations when compared with highly crystalline interfaces. Here, we performed density functional calculations of our Cu(111)/α-Bi$_2$O$_3$ [13]. Figure 1(a) shows the calculated layer-projected density of states (LDOS) at the Cu(111)/α-Bi$_2$O$_3$ interface (dashed line zone) and its vicinity. At the interface, it is possible to observe a modification of the LDOS at both sides close to the interface, corresponding to Cu and Bi$_2$O$_3$ hybridization of Cu-O-Bi states due to charge transfer. We sketched the calculated charge density of a Rashba state of the Cu(111)/α-Bi$_2$O$_3$ interface in Fig. 1(b), where blue, red, and purple spheres are Cu, O, and Bi atoms, respectively; yellow clouds represent the Cu-O-Bi states.

Band structure analysis around the C point of states below the Fermi level shows a Rashba-like band splitting; see Fig. 1(c). We evaluated Rashba parameters at the C point (0.5, 0.5) in the unit of two-dimensional reciprocal lattice vectors. From the spin split energy band dispersion, the Rashba parameter is calculated by using an expression $\alpha_R = 2E_R/k_R$, where E_R is the Rashba energy and k_R is the Rashba momentum offset [22]. The averaged Rashba coefficient $\alpha_R = 0.91 \times 10^{-10}$ eV m accounts for the energy band spin splitting around the Fermi energy as shown in Fig. 1(c), which is the same order of magnitude of values reported by spin-to-charge conversion [7,8]. Remarkably, around 1.98 eV above the Fermi level we
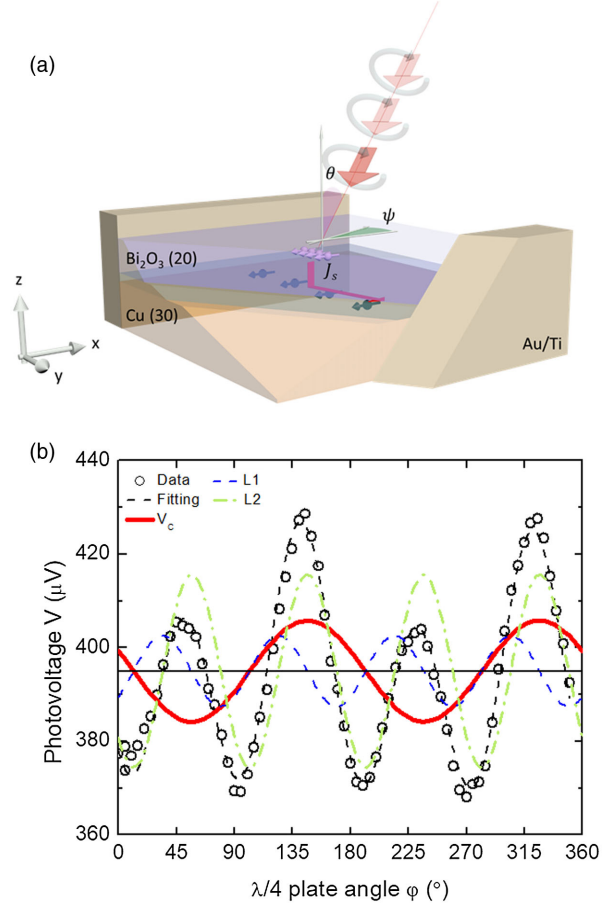
locate another Rashba splitting of an unoccupied state. The averaged Rashba coefficient $\alpha_R = 1.72 \times 10^{-10}$ eV m accounts for the large energy band spin splitting around 1.98 eV above the Fermi energy as shown in Fig. 1(d), almost two times larger than that observed around the Fermi level. The energy of this unoccupied state with Rashba splitting is in close proximity to the well-known interband transition energy between d states and s states of Cu, with both states participating at the interfacial hybridization.

We test the photoinduced Rashba spin-to-charge conversion with excitation energy of 1.96 eV at room temperature. The configuration of our photoinduced spin-to-charge conversion experiment is sketched in Fig. 2(a). We generate spin currents by the absorption of angular

momentum from light, via the photovoltaic conversion. The angular momentum of light is dictated by its degree of circular polarization or helicity. Notice that, unlike standard heterostructures for photovoltaic devices where photovoltaic collection occurs at the bottom and top electrodes, in our device the photovoltaic collection occurs in transverse geometry, following the inverse Edelstein effect (IEE) spin-to-charge conversion, $E \approx \sigma_s \times J_s$ [7,8,23], where σ_s is the vector of spin polarization and J_s is the flow direction of the spin current. The interface is formed between a 30 nm thick Cu layer and 20 nm thick Bi_2O_3. These thicknesses are selected to suppress interaction of the Si/SiO_2 substrate and the excitation light. The laser beam has an incidence angle θ and an azimuthal angle Ψ. The photon polarization is controlled by a linear polarizer and a quarter wave plate mounted on a rotator.

In Fig. 2(b), we show the helicity dependent photovoltaic measurement obtained with excitation laser energy of 1.96 eV. Changing the contributions of polarized light due to the rotation of the quarter wave plate (φ) leads to periodic modulation in photovoltage with a periodicity of 90°. Photovoltage peaks have different amplitudes, showing periodically two different values. This asymmetry comes from the circularly polarized light modulation analogous to the circular photogalvanic effect [24]. To better describe the contributions in our modulated signal, we fit the data with the following phenomenological formula [25,26].

$$V_{\text{out}} = V_C \sin(2\varphi) + L_1 \sin(4\varphi) + L_2 \cos(4\varphi) + A. \quad (1)$$

Here, V_C represents the amplitude associated with the degree of circular polarization of light or helicity (red solid line in Fig. 2), L_1 is the amplitude associated with the linear polarization of light (blue dashed line in Fig. 2), L_2 depends on the Fresnel coefficients [27] (green dashed line in Fig. 2) and A is a nonmodulated photovoltage offset independent of light polarization. From the fitting we can obtain the amplitude of the photovoltage V_{out}, which depends exclusively on the helicity of light V_C, and estimate the optical generated spin current by [8,23]

$$J_s = \frac{V_C}{\lambda_{\text{IEE}}\omega R}, \quad (2)$$

where λ_{IEE} is the inverse Edelstein effect length directly proportional to the Rashba parameter by $\lambda_{\text{IEE}} = (\alpha_R \tau_e)/\hbar$, τ_e is the momentum relaxation time governed by Cu [7,12], ω is the width of our interface, and R is the sample resistance. We estimate the spin current by taking the voltage due to circular polarization from fitting of Fig. 2(b), $V_C = 10.8 \times 10^{-6}$ V, $\lambda_{\text{IEE}} = 2.35 \times 10^{-9}$ m, $\omega = 0.9 \times 10^{-3}$ m, and $R = 4.8$ Ω giving a resistivity $\rho = 8.64$ $\mu\Omega$ cm, we obtain $J_s = 1.06 \times 10^6$ A/m^2, a value comparable with the spin current commonly generated by
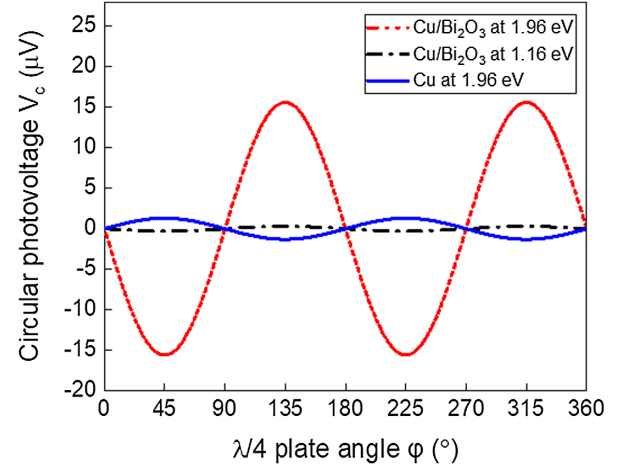

FIG. 3. Comparison of circularly polarized voltage V_C. Circular photovoltage conversion of $Cu(111)/\alpha$-Bi_2O_3 at 1.96 eV (red dashed line) is dramatically larger than circular photovoltage conversion at 1.16 eV (black dash-dot line), reflecting a threshold energy. Circular photovoltage conversion at 1.96 eV of $Cu(111)/\alpha$-Bi_2O_3 (red dashed line) is significantly larger than circular photovoltage conversion in Cu (blue solid line), reflecting the necessity of an interface with charge transfer and Rashba splitting.

spin pumping experiments [8,23] and previous reports of circular photovoltaic conversion by inverse spin Hall effect [28,29]. This estimation is valid when the contribution from the Schottky barrier is negligible. Such is the case for our $Cu(111)/\alpha$-Bi_2O_3 [13].

In further scrutiny, Fig. 3 compares V_C generation in three scenarios: excitation of $Cu(111)/\alpha$-Bi_2O_3 by 1.96 eV (red dashed line), 1.16 eV (black dash-dot line) energy lasers, and excitation of only the Cu layer at 1.96 eV (blue solid line), at $\theta = 70°$ and $\Psi = 0°$. Figure 3 shows that V_C (1.96 eV) $\gg V_C$ (1.16 eV) for $Cu(111)/\alpha$-Bi_2O_3, indicating drastic suppression of the detected photovoltage coming from the circular polarization of light at 1.16 eV, and also showing negligible contribution of circular polarized photovoltage coming from the Si substrate, which has a band gap of 1.10 eV. We also observe that V_C [$Cu(111)/\alpha$-Bi_2O_3] $\gg$ V_C [$Cu(111)$] with excitation at 1.96 eV, indicating the relevance of the $Cu(111)/\alpha$-Bi_2O_3 interface. Moreover, we observe an opposite phase of spin-to-charge conversion for $Cu(111)/\alpha$-Bi_2O_3 and $Cu(111)$, in agreement with the opposite sign of spin-to-charge conversion between $Cu(111)/\alpha$-Bi_2O_3 [7–9] and the recent reports of conversion of the natural oxide in Cu [14].

First-principles calculations showed hybridization of Cu-O-Bi charge states at our interface and Rashba splitting around 1.98 eV above the Fermi energy, allowing the interfacial charge separation mechanism and IEE spin-to-charge conversion. Transverse photovoltage induced by circular polarized light can also be generated in surface state polaritons via an asymmetric variation of the photon drag effect [30,31]. This mechanism requires only surface
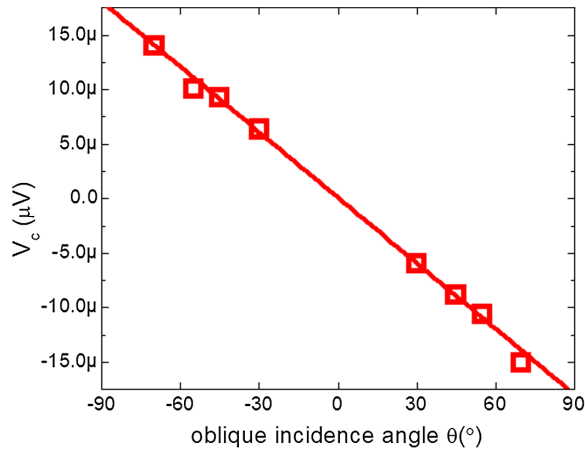
FIG. 4. Oblique incidence dependence of circularly polarized voltage V_C. Circular photovoltage conversion of Cu(111)/α-Bi$_2$O$_3$ at 1.96 eV (red dashed line) increases with the projection onto the interface plane, and changes its sign at opposite oblique incidence angles as expected in a spin-to-charge conversion mechanism.

state plasmons in metals and not necessarily the assistance of a semiconductor such as the plasmon induced hot electrons mechanism [32,33]. We tested the response of a Cu (111) layer to circular polarized light at 1.96 eV. While Cu (111) preserved the optical absorption due to the Shockley surface states, we do not observe significant transverse photovoltage related to circular polarized light, therefore, further suggesting the combination of interfacial induced charge transfer and IEE as the origin for our circular polarized photovoltage at the Cu(111)/α-Bi$_2$O$_3$ interface.

Finally, we study the oblique incidence angle dependence of our photoinduced spin-to-charge conversion (see Fig. 4). The oblique incidence dependence shows an increase of circular photovoltaic signal as the projection is increased onto the plane, and reverses its sign at opposite oblique incidence angles, following spin-to-charge conversion mechanisms. The interpretation of our data works under the assumption of an interband transition of the d states to the partially filled s states of Cu, as suggested by the typical interband optical absorption, the hybridization of our first-principles analysis, and the prediction of a Rashba splitting of states at 1.98 eV above the Fermi level.

To summarize, we showed the spin photovoltaic conversion at the Cu(111)/α-Bi$_2$O$_3$ interface. Because of the increasing number of interfaces with broken spatial inversion symmetry [3,7–11], we expect that the present work motivates further studies, advancing conversion efficiencies and understanding towards spin orbitronics in photovoltaics [34]. From our present and previous reports, we have indication of spin-to-charge conversion at the Cu(111)/α-Bi$_2$O$_3$ interface due to Rashba spin orbit coupling [7–10,23]. Rashba spin orbit coupling is suggested as a key component to suppress carrier recombination and enhanced carrier lifetime in perovskites [35,36].

We observed an efficient photovoltaic conversion arising from a charge transfer mechanism at our Cu(111)/α-Bi$_2$O$_3$ interface and Rashba spin splitting in an excited state. The photoinduced spin-to-charge conversion via Rashba spin splitting in an excited state motivates further studies in similar structures, and further understanding of the mechanism involved. Very recently, a related report shows circular photovoltaic signal at metal-metal interface [37], the interpretation of our results may shed new light in the understanding of this recent report and motive further studies. Our device is compatible with complementary metal-oxide-semiconductor (CMOS) technology, opening a new venue for exploring spin orbitronics at interfaces towards spin electronic devices beyond Moore's law [38].

[*]jorgeluis.pueblanunez@riken.jp
[†]yotani@issp.u-tokyo.ac.jp

[1] Y. Otani, M. Shiraishi, A. Oiwa, E. Saitoh, and S. Murakami, Spin conversion on the nanoscale, Nat. Phys. **13**, 829 (2017).

[2] A. Manchon, H. C. Koo, J. Nitta, S. M. Frolov, and R. A. Duine, New prespectives for Rashba spin-orbit coupling, Nat. Mater. **14**, 871 (2015).

[3] Y. Ando and M. Shiraishi, Spin to charge interconversion phenomena in the interface and surface states, J. Phys. Soc. Jpn. **86**, 011001 (2017).

[4] H. Liang, L. Cheng, L. Wei, Z. Luo, G. Yu, Ch. Zeng, and Z. Zhang, Nonmonotonically tunable Rashba spin-orbit coupling by multiple-band filling control in SrTiO$_3$-based interfacial d-electron gases, Phys. Rev. B **92**, 075309 (2015).

[5] G. Herranz, G. Singh, N. Bergeal, A. Jouan, J. Lesueur, J. Gázquez, M. Varela, M. Scigaj, N. Dix, F. Sánchez, and J. Fontcuberta, Engineering two-dimensional superconductivity and Rashba spinorbit coupling in LaAlO$_3$/SrTiO$_3$ quantum wells by selective orbital occupancy, Nat. Commun. **6**, 6028 (2015).

[6] K. Kondou, R. Yoshimi, A. Tsukazaki, Y. Fukuma, J. Matsuno, K. S. Takahashi, M. Kawasaki, Y. Tokura, and Y. Otani, Fermi-level-dependent charge-to-spin current conversion by Dirac surface states of topological insulators, Nat. Phys. **12**, 1027 (2016).

[7] H. Tsai, S. Karube, K. Kondou, N. Yamaguchi, F. Ishii, and Y. Otani, Clear variation of spin splitting by changing

electron distribution at non-magnetic metal/Bi_2O_3 interfaces, Sci. Rep. **8,** 5564 (2018).

[8] M. Xu, J. Puebla, F. Auvray, B. Rana, K. Kondou, and Y. Otani, Inverse Edelstein effect induced by magnon-phonon coupling, Phys. Rev. B **97,** 180301(R) (2018).

[9] J. Puebla, F. Auvray, M. Xu, B. Rana, A. Albouy, H. Tsai, K. Kondou, G. Tatara, and Y. Otani, Direct optical observation of spin accumulation at nonmagnetic metal/oxide interface, Appl. Phys. Lett. **111,** 092402 (2017).

[10] F. Auvray, J. Puebla, M. Xu, B. Rana, D. Hashizume, and Y. Otani, Spin accumulation at nonmagnetic interface induced by direct Rashba-Edelstein effect, J. Mater. Sci. Mater. Electron., **29,** 15664 (2018).

[11] C. J. Li, Y. P. Hong, H. X. Xue, X. X. Wang, Y. Li, K. Liu, W. Jiang, M. Liu, L. He, R. F. Dou, C. M. Xiong, and J. C. Nie, Formation of two-dimensional electron gas at amorphous/crystalline oxide interfaces, Sci. Rep. **8,** 404 (2018).

[12] J. M. Flores-Camacho, J. Puebla, F. Auvray, Y. Otani, and R. E. Balderas-Navarro, Two-dimensional electron gas in a metal/amorphous oxide interface with spin orbit interaction, arXiv:1901.08671.

[13] See Supplemental Material at http://link.aps.org/supplemental/10.1103/PhysRevLett.122.256401 for device fabrication and experimental setup methods, first-principles calculation details, additional data fittings, *I-V* characteristics, absorption, and x-ray spectroscopy, which includes Refs. [14–21].

[14] H. An, Y. Kageyama, Y. Kanno, N. Enishi, and K. Ando, Spin-torque generator engineered by natural oxidation of Cu, Nat. Commun. **7,** 13069 (2016).

[15] T. Ozaki, Variationally optimized atomic orbitals for large-scale electronic structures, Phys. Rev. B **67,** 155108 (2003).

[16] T. Ozaki and H. Kino, Efficient projector expansion for the *ab initio* LCAO method, Phys. Rev. B **72,** 045121 (2005).

[17] J. Perdew, K. Burke, and M. Ernzerhof, Generalized Gradient Approximation Made Simple, Phys. Rev. Lett. **77,** 3865 (1996).

[18] G. Theurich and N. A. Hill, Self-consistent treatment of spin-orbit coupling in solids using relativistic fully separable *ab initio* pseudopotentials, Phys. Rev. B **64,** 073106 (2001).

[19] T. Ozaki and H. Kino, Numerical atomic basis orbitals from H to Kr, Phys. Rev. B **69,** 195113 (2004).

[20] M. Otani and O. Sugino, First-principles calculations of charged surfaces and interfaces: A plane-wave nonrepeated slab approach, Phys. Rev. B **73,** 115407 (2006).

[21] T. Ohwaki, M. Otani, T. Ikeshoji, and T. Ozaki, Large-scale first-principles molecular dynamics for electrochemical systems with O(N) methods, J. Chem. Phys. **136,** 134101 (2012).

[22] K. Ishizaka *et al.*, Giant Rashba-type spin splitting in bulk BiTeI, Nat. Mater. **10,** 521 (2011).

[23] J. C. Rojas-Sanchez, L. Vila, G. Desfonds, S. Gambarelli, J. P. Attane, J. M. De Teresa, C. Magen, and A. Fert, Spin-to-charge conversion using Rashba coupling at the interface between non-magnetic materials, Nat. Commun. **4,** 2944 (2013).

[24] S. D. Ganichev and W. Prettl, Spin photocurrents in quantum wells, J. Phys. Condens. Matter **15,** R935 (2003).

[25] H. Yuan *et al.*, Generation and electric control of spinvalley-coupled circular photogalvanic current in WSe_2, Nat. Nanotechnol. **9,** 851 (2014).

[26] D. Niesner, M. Hauck, S. Shrestha, I. Levchuk, G. J. Matt, A. Osvet, M. Batentschuk, C. Brabec, H. B. Weber, and T. Fauster, Structural fluctuations cause spin-split states in tetragonal $(CH_3NH_3)PbI_3$ as evidenced by the circular photogalvanic effect, Proc. Natl. Acad. Sci. U.S.A. **115,** 9509 (2018).

[27] K. N. Okada, N. Ogawa, R. Yoshimi, A. Tsukazaki, K. S. Takahashi, M. Kawasaki, and Y. Tokura, Enhanced photogalvanic current in topological insulators via Fermi energy tuning, Phys. Rev. B **93,** 081403(R) (2016).

[28] G. Isella, F. Bottegoni, A. Ferrari, M. Finazzi, and F. Ciccacci, Photon energy dependence of photo-induced inverse spin-Hall effect in Pt/GaAs and Pt/Ge, Appl. Phys. Lett. **106,** 232402 (2015).

[29] K. Ando, M. Morikawa, T. Trypiniotis, Y. Fujikawa, C. H. W. Barnes, and E. Saitoh, Photoinduced inverse spin-Hall effect: Conversion of light-polarization information into electric voltage, Appl. Phys. Lett. **96,** 082502 (2010).

[30] T. Hatano, T. Ishihara, S. G. Tikhodeev, and N. A. Gippius, Transverse Photovoltage Induced by Circularly Polarized Light, Phys. Rev. Lett. **103,** 103906 (2009).

[31] K. Y. Bliokh and F. Nori, Transverse spin of a surface polariton, Phys. Rev. A **85,** 061801(R) (2012).

[32] T. Tatsuma, H. Nishi, and T. Ishida, Plasmon-induced charge separation: Chemistry and wide applications, Chem. Sci. **8,** 3325 (2017).

[33] C. Clavero, Plasmon-induced hot-electron generation at nanoparticle/metal-oxide interfaces for photovoltaic and photocatalytic devices, Nat. Photonics **8,** 95 (2014).

[34] K. Amnuyswata and P. Thanomngam, Roles of spin-orbit coupling in tetragonal hybrid halide perovskite for photovoltaics light-absorber, Mater. Today: Proc. **5,** 14857 (2018).

[35] J. Even, L. Pedesseau, J-M Jancu, and C. Katan, Importance of spinorbit coupling in hybrid organic/inorganic perovskites for photovoltaic applications, J. Phys. Chem. Lett. **4,** 2999 (2013).

[36] F. Zheng, L. Z. Tan, S. Liu, and A. M. Rappe, Rashba spinorbit coupling enhanced carrier lifetime in $CH_3NH_3PbI_3$, Nano Lett. **15,** 7794 (2015).

[37] H. Hirose, N. Ito, M. Kawaguchi, Y. C. Lau, and M. Hayashi, Circular photogalvanic effect in Cu/Bi bilayers, Appl. Phys. Lett. **113,** 222404 (2018).

[38] S. Manipatruni, D. E. Nikonov, and I. A. Young, Beyond CMOS computing with spin and polarization, Nat. Phys. **14,** 338 (2018).